

August 18, 2003

RUNNING HEAD: AUTOMATED MEASUREMENT OF *DROSOPHILA* WINGS

Automated Measurement of *Drosophila* Wings

David Houle^{*,†,‡}, Jason Mezey[†], Paul Galpern^{*} and Ashley Carter[†]

**Department of Zoology, University of Toronto, Toronto, Ontario M5S 3G5 Canada*

†Department of Biological Science, Florida State University, Tallahassee, Florida, 32306 USA

‡ dhoule@bio.fsu.edu

Correspondence to:

David Houle

Dept. of Biological Science

Florida State University

Tallahassee, FL 32306-1100

Tel: 850-645-0388

FAX: 850-644-9829

E-mail: dhoule@bio.fsu.edu

Submitted to Systematic Biology

ABSTRACT

We have developed an automated image analysis system (WINGMACHINE) that enables rapid, highly repeatable measurements of wings in the family Drosophilidae. A simple suction device allows video images to be taken of the wings of live flies. Low-level processing is used to find the major intersections of the veins. High-level processing then optimizes the fit of an *a priori* model of wing shape. The result is a B-spline approximation to the positions of all the veins and the edges of the wing blade that utilizes 50 control points. The combination of handling, imaging, analysis, and editing of the resulting data has been reduced to an average of about 1 minute per wing. The repeatabilities of 12 vein intersections averaged 86% in a sample of flies of the same species and sex. Comparison of 2400 wings of 24 Drosophilid species shows that wing shape is quite conservative within the group, but that almost all taxa are diagnosably different from one another. UPGMA clustering of the species suggests that wing shape retains some phylogenetic structuring, although some species have shapes very different from closely related species. The WINGMACHINE system facilitates artificial selection experiments on complex aspects of wing shape. We selected on an index which is a function of 14 separate measurements of each wing. After 14 generations, we achieved a 15 S.D. difference between up and down-selected treatments. Our approach to image analysis may be applicable to a variety of biological objects that can be represented as a framework of connected lines. The use of high-level analysis based on a priori information about shape deserves much wider application in morphometrics.

Keywords: [Morphometrics; image analysis; wing venation; Drosophilidae; morphological evolution.]

Many endeavors in biology are limited by a combination of the number of specimens that can be measured, and the amount of information that can be extracted from each one. Examples include biodiversity surveys (Weeks and Gaston, 1997), quantitative trait locus studies (Liu et al., 1996), and artificial selection experiments (Weber and Diggins, 1990). Consequently, automated methods for measuring the morphology of specimens have long been desired by systematists, geneticists and evolutionary biologists.

Advances in technology and manufacturing of digitizing equipment and video cameras have greatly increased the ease with which landmarks or outlines can be recorded, especially in organisms (or parts thereof) where the specimen is readily projected into two dimensions (Rohlf, 1993). In some cases, the combination of specimen handling, imaging and feature extraction can be very rapid. Good examples include the extraction of outlines from high contrast objects such as leaves (Jensen et al., 2002) or shells (Ferson et al., 1985). In many other cases internal details of a specimen are of primary interest, or the form of the organism precludes such a simple approach. Sophisticated automated systems have been devised to extract such information (Zhou et al., 1985), but none appear to have been widely used. As a result, in the vast majority of morphometric studies, considerable effort on the part of the observer is still required in the measurement of each specimen. Despite the fact that digitization is far quicker than manual measurement and recording of data, it can still be the limiting step in many morphometric studies. The preparation of the specimen for measurement may also be quite time-consuming.

Here we report on our largely automated system for recovering the locations of wing veins of flies in the family Drosophilidae. Drosophilid wings are an unusually favorable subject for automated image analysis. This is first because of the wealth of interesting and accessible

biological questions that can be addressed with their wings. The function of wings for flight is clear, although they also function as sense organs (Dickinson et al., 1997), and in courtship. The nominate genus *Drosophila* includes the model organism *D. melanogaster*, as well as many other species that are preadapted to laboratory culture. Second, Drosophilid wings are quite easy to measure and handle because they are two-dimensional, translucent and relatively sturdy, having evolved to withstand large forces. As a result of these factors, Drosophilid wings are widely used for the study of the genetics of development, morphometrics and evolution (e.g. (Cowley et al., 1986; Garcia-Bellido and de Celis, 1992; Stark et al., 1999; Gilchrist et al., 2000; Klingenberg and Zaklan, 2000)).

The current standard approach to the measurement of *Drosophila* wings is to mount detached wings, then digitize the positions of vein intersections manually (e.g. Klingenberg and Zaklan, 2000; Zimmerman et al., 2000). Weber (1988) devised a complex apparatus to immobilize the wing of a live, intact fly, and project its image onto a digitizing tablet, thereby shortening handling time. Using this apparatus, Weber was able to perform a comprehensive series of selection experiments that demonstrated that the wings of *D. melanogaster* could readily evolve counter to the allometry within the species (Weber, 1990, 1992).

In this paper we describe the hardware and software that together make up the automated wing measurement system, which we call WINGMACHINE. The WINGMACHINE allows the measurement of 100 pieces of information from the wing of a living specimen in one every minute. Our approach to feature extraction is unusual in basic biological applications in employing an *a priori* model as part of feature extraction. We report the repeatability of the resulting data, and briefly describe results from comparison of species and an artificial selection

experiment.

SPECIMEN HANDLING

To handle specimens, we devised the simple ‘wing grabber’ suction device shown in Fig. 1. This is a simplified version of the apparatus used by Weber (1988). Vacuum is provided by a small pump (1/8hp 22 l/min Welch dry vacuum pump 2522B-01). The flies to be measured are anaesthetized on a standard CO₂ stage. The operator then takes the wing grabber in one hand, while maneuvering the target fly with a small paintbrush in the other hand. Once the wing grabber is properly positioned with the slit directly behind the fly and parallel to its wings, the operator places one finger over the top hole of the grabber, increasing the suction through the slit and sucking one wing into the grabber. Releasing and recovering the opening permits repositioning of the fly until a single wing is clearly visible, as shown in Fig. 2a. The wing grabber with attached fly is then positioned on the stage of a macroscope (see below) and a video image recorded. When suction is relaxed, the fly is pulled from the wing holder and put aside to recover consciousness. This operation takes a few seconds, so the fly is still anaesthetized despite being removed from the CO₂ flow. Operators usually become moderately proficient at this operation after a few trials, and expert with a few hours of experience. The amount of vacuum is adjusted to a level where the wing is readily grabbed without folding the wing by varying the input of the pump or the width of the slit.

After a few hours of operation, the slide and coverslip become too dirty for further use.

At this point, the brass fitting is detached from the putty holding it in place, and a clean cover slip

is attached to a new slide using fresh double-sided tape. A ring of putty is then placed over the gap between slide and coverslip and the brass fitting reattached.

IMAGING

We have constructed three imaging systems with different hardware and front-end software programs. The key requirements of the system are that it produce a monochrome digital image, record two landmark locations and associate both with other recorded information about the specimen. To calibrate the size of the image, a stage micrometer is digitized before wings are imaged.

Both of our current systems use an Optem Zoom100 macroscope interfaced with ½ inch monochrome CCD video cameras and a frame grabber board in a Windows computer.

Recording information about each image requires programmable software. ImagePro Plus 4.0 (Media Cybernetics, 1999), an expensive image analysis program that includes a full-featured C-based programming language, is readily adapted for this purpose. In addition, we also use Scion Image (Scion Corporation, 2001), the commercial Windows version of NIH Image. While Scion Image is available without charge, it can only be used with a Scion frame grabber board. Scion Image has very minimal programming and output capability, so recording specimen information requires the use of a companion C++ program we have written.

Once an image is obtained, contrast is adjusted using the automatic algorithm in each software package. The operator then records the positions of two landmarks, the distal edge of the humeral break, and the tip of the fissure between the alula and the posterior edge of the wing

blade. The recording programs automatically zoom the image to these areas in turn to improve accuracy. The image is saved as a TIFF file, and the associated identification, landmark coordinates and scale information written to another file.

FEATURE EXTRACTION

The heart of the image analysis system is a C program called FINDWING, which takes the TIFF image and the associated coordinate information and produces a cubic B-spline approximation to the position of all the wing veins distal to the line between the user-supplied landmarks, as shown in Fig. 2f. The key to the success of this algorithm is its use of an *a priori* B-spline model (Lu and Milios, 1994) which is matched to the image of the wing. An example of this model is shown in Fig. 3. B-splines do not pass through their control points (shown as squares in Fig. 3), although they do pass through a point half way between adjacent control points. By convention, the end of the spline curve is represented as a control point (shown as circles in Fig. 3), and the interpolating function adjusted to compensate.

FINDWING combines basic image processing of the wing image to facilitate the registration and modification of the *a priori* model. FINDWING proceeds in four major steps: preprocessing, production of a skeletonized binary representation, registration of the intersections of the skeleton with the joins in the *a priori* model, and fitting of each spline curve to the preprocessed image. These steps are illustrated in Fig. 2.

In the preprocessing step, the raw image matrix (Fig. 2a) is inverted, subjected to a 3X3 median filter, and then subtraction of a gray scale opening (an erosion, followed by dilation using

the same dimension of operator) to obtain the image Fig. 2b. These two operations largely remove small-scale features that form the uninformative background of the image. This matrix is used as input for both the skeletonization and fitting steps below.

To obtain a skeletonized binary image, the preprocessed matrix is thresholded, holes between features filled (Fig. 2c), the resulting features skeletonized (Fig. 2d), then short line segments are removed (Fig. 2e). The parameters of each of these operations, such as the size of the opening filter and the cutoff for thresholding are under the control of the operator. The intersections (joints) of the remaining lines in this step are used as input for the registration step.

For registration, the image is first flipped to the standard orientation shown in Fig. 2 if necessary. Each observed joint is then tested to see if it is far enough from the landmark at 6 to potentially be either point 1 or 2. If it is, then the direction from the joint to landmark is used to define an affine transformation (translation, rotation, x and y scaling and shear) of all the observed joints. The nearest joint to the set of reference joints in this transformed space is then tentatively assigned the identity of that point, and the least squares deviation of this configuration from the model computed. The affine transformation that results in the best fit by least squares is then assumed to be the correct one. Reference systems based on both points 1 and 2 are evaluated in this way to guard against the case where no joint corresponding to one of these points is detected.

Finally, from the starting point defined by the best affine transformation of the model, the fit of each of the nine model curves is optimized using an approach based on that of Lu and Milios (1994). This approach treats the coordinates of the control points as variables, and does not fix the locations of the knots. The fit of the curve is optimized by maximizing the brightness

of the pixels under the curve in the inverted image (Fig. 2b). The brightness (b , range 0 to 255) of each pixel is transformed to “energy” E as $E_{\bar{y}} = 255 \exp[-0.12b_{\bar{y}}]$, and this matrix smoothed. The energy of a spline curve is the sum of the energy of each point under the curve. This energy is maximized by solving for the gradient vector of each control point with respect to E , then updating the set of control points using a variable step size. When this step converges to a solution, the resulting set of 100 parameters is output.

The output of FINDWING is a file giving the model parameters for each wing, and a TIFF image with the model overlaid on the raw image (Fig. 2f). This model is readily used to solve for derived measurements of any aspect of wing form defined by the model. We have principally analyzed the locations of vein intersections using a geometric morphometric approach, but any parameters measurable from the original vein structure, such as lengths, perimeters, areas or angles, can be recovered from the model.

The fitting parameters currently implemented in FINDWINGS work well on monochrome images that are 316 by 240 pixels. We expect that parameters giving good fits for other image sizes could be found, although we have not yet done so.

RUNNING FINDWING

The success of FINDWING in fitting a model depends on the initial model parameters furnished the program, and a large set of fitting parameters that can be altered by the user. To maximize the success of the splining process, the model and fitting parameters often must be altered for

each batch of wings according to species or lighting conditions. Finding an appropriate set of parameters is a matter of trial and error, aided by examining the results of intermediate processing steps (Fig. 2). Fitting parameters that are frequently altered include the dimension of the open radius used in preprocessing, and the threshold used to create the binary image for skeletonization. The same model parameters are frequently successful for species with similar wing shapes. When a new model is needed, it is usually quite easy to find, as even a poor set of initial model parameters will result in a good fit to a minority of wings in a sample. Use of any of these successful output parameter sets as the initial model usually results in suitable fit to the majority of images in subsequent runs. Alternatively, a new model can be created by digitizing a likely set of control points, based on the properties of B-splines (Fig. 3).

We use FINDWING for both batch processing of large sets of wings, and for real-time interactive processing of single wings. When the goal of a study is to characterize variation among individuals or taxa, batch processing is more rapid than real-time processing. Real-time processing is convenient during a selection experiment, where a decision about whether to use an individual as a parent must be made rapidly. An important advantage of real time processing is that the operator can immediately examine the fit and if necessary alter the fitting parameters and rerun FINDWING until a suitable fit is achieved. The cost is the time that the operator puts into this checking and rerunning process. The run time of FINDWING itself is less than a second per wing on current Windows-based processors. In batch mode, one set of fitting parameters will typically produce excellent fits for 95 to 98% of the specimens. When used in batch mode, an experienced operator can image about 1 fly every 40 seconds. In real-time applications, this is slowed to about 1 fly per minute.

When processing wings in batch mode, an important challenge is finding those cases when the fit of the model to the image is deficient. In all batch applications, we have been interested in the coordinates of landmark points, rather than curve locations per se. Since the vast majority of wings spline properly, examining each image is exceptionally tedious. To automate this process, we examine only multivariate outliers. The locations of the twelve labeled landmarks shown in Fig. 3 are first identified as the intersections of the appropriate model curves. Landmark coordinates are then aligned using the generalized least squares fit in tpsRegr (Rohlf, 1998b). Potential outliers are then flagged with Rousseeuw's minimum volume ellipsoid (MVE) algorithm (Rousseeuw, 1985; Rousseeuw and van Zomeren, 1990), as implemented in the S-Plus program cov.mve (Insightful Corporation, 2001a). MVE uses the Mahalanobis distance based on a robust estimate of the covariance matrix to detect outliers, thus preventing outliers from masking their own presence. The unaligned landmark coordinates from each outlier model are displayed along with the raw wing image in the digitizing program tpsDig (Rohlf, 1998a), and landmarks dragged to their proper locations using a mouse, if necessary. This procedure finds both abnormal wings and cases where the model does not fit well.

Real-time processing is currently implemented through the C++ program SELECTOR that uses the output of a Scion Image macro and runs FINDWING and ACDSee, a tiff viewer (ACD Systems, 2001). Batch processing is implemented through a series of S-Plus scripts (Insightful Corporation, 2001b) that spawn the necessary programs FINDWING, ACDSee, tpsRegr and tpsDig. These scripts are currently being ported to R, the share-ware implementation of S. Compiled code for FINDWING, the S-Plus scripts, and example data are available at <http://www.bio.fsu.edu/~dhoule/Software/>. The source code for FINDWING is

available from the first author.

REPEATABILITY

To assess the repeatability of the WINGMACHINE system, we repeatedly imaged and analyzed the wings of *Drosophila melanogaster* generated as part of a much larger quantitative genetic study (Mezey and Houle, 2003). One hundred thirty-five *D. melanogaster* females were captured in Wabasso, Florida in March 2002 and their offspring pooled to form a laboratory population. In August 2002, five males from this population were each mated to three virgin females, and their offspring reared on standard cornmeal-sucrose-brewer's yeast medium at 25°C. A sample of offspring from these crosses were measured over a period of 9 days by five operators. Flies were measured between 2 and 11 days of adult age. In each case, the upper side of the left wing was imaged. Male flies (N=87) were imaged an average of 3.3 times, and female flies (N=92) an average of 2.7 times each, for a total of 535 wing images.

Variance component estimates for each sex separately showed that the variances did not differ significantly, so the sexes were analyzed together. Variance components for centroid size and the coordinates of the 12 landmarks were estimated in the SAS program MIXED (Littell et al., 1996; SAS Institute, 2002), with sex as a fixed effect and fly and operator as random effects. Variance components for the x and y coordinates of each point were summed to obtain the point variance estimates shown in Table 1. Significance of the main effects at each point was tested by MANOVA in GLM (SAS Institute, 2002).

As expected, female wings are on average larger than male wings (centroid size 1201 vs.

1036 μm), and the mean location of all of the landmarks also differs between the sexes at $P < 0.0001$. The repeatability of centroid size within sexes is very high at 96%. Table 1 also shows the among fly variance component over sexes, and the proportion of the within-sex variance that this represents. The average repeatability over all 12 points is 82%. The least repeatable points also tend to have the least variance, so the proportion of the total variance in locations that is fly variance is a little higher at 86%. Point 5 is the least accurately captured (repeatability 47%), which is not surprising as this curve does not follow the entire length of the costal vein. This was a deliberate choice in the design of the program, as there is a large break at the end of the costa that is quite difficult to spline around. When point 5 is removed from consideration, the average repeatability rises to 85%. Operator effects are significant for the majority of the points, but represent less than 1% of the total variation among images. Point 6, one of the initial landmarks entered by the operator, has the largest operator effect, but this is still only 3.2% of the total.

Another potential source of error is the choice of the initial model and fitting parameters. To investigate this, we took the images from the above data set measured by one operator ($N=179$), and splined and corrected them using two different sets of initial model parameters and four different sets of fitting parameters in a total of five combinations. After the editing process, repeatabilities across this set of measurements are considerably higher, totaling 93%, as shown in the final column of Table 1. Mean differences among parameters are slight, and generally not significant. Even when models based on the wings of three different species are used for the initial models (*D. melanogaster*, *virilis*, and *affinis*), total repeatability only declines to 91%. As above, points 5, 11 and 12 again have relatively low repeatabilities.

SPECIES DATA

One important use of high dimensional phenotypic data that an automated system can produce is investigation of the relationship between phylogeny and phenotypic evolution. For example, discrepancies between phenetic and phylogenetic relationships may indicate taxa where evolution has been unusually rapid or unusual in some other way.

To investigate the ability of the wing machine system to measure other species, we imaged individuals of 24 species in the sub-family Drosophilinae of the family Drosophilidae, listed in Table 2. Species were chosen to represent a wide diversity of taxa in the traditional genus *Drosophila*, along with a few outgroup taxa. Stocks were obtained through collection, or through the *Drosophila* Species Stock Center, then at Bowling Green. Specimens were mostly reared in our laboratory on either cornflour-sucrose, or banana-molasses medium according to the recommendations of the Stock Center (currently at <http://stockcenter.arl.arizona.edu/>).

Individuals of *Scaptodrosophila stonei*, *Zaprionus sepsoides*, *Z. inermis* and *D. micromelanica* did not reproduce in our hands, and so wings of individuals emerging from vials sent by the stock center were imaged. Individuals of *D. melanogaster* were drawn from two populations: a wild collection from Whitby, Ontario Canada; and a long-term laboratory population (IV) (Houle and Rowe, 2003). All specimens were imaged and splined by one operator. Splining model and fitting parameters were adjusted for each species to maximize the success rate as judged by the operator. The result was that a different model was used for each species. Discriminant analysis was carried out in Proc Discrim in SAS (SAS Institute, 2002), while UPGMA was carried out with “agnes” in S-Plus (Insightful Corporation, 2001a).

Despite the great interest in the genus *Drosophila* as a model for genetics, development and evolution, there is still considerable doubt over the correct phylogeny within the genus and the Drosophilinae. Fig. 4 presents a phylogenetic hypothesis for the taxa in our sample, showing some major unresolved issues. The consensus phylogeny of Remsen and O'Grady (Remsen and O'Grady, 2002) was used as the basis for the hypothesis, supplemented by other results for the more closely related taxa (Powell and DeSalle, 1995; Tatarenkov and Ayala, 2001; O'Grady and Kidwell, 2002).

The aligned and size-adjusted landmark coordinates for all 2406 individuals measured are shown in Fig. 5. Overall, the positions of landmarks are quite conservative, with considerable overlap in landmark positions among species. Wing shape in the Drosophilinae provides an example of relative stasis.

Despite the impression of stasis, linear discriminant analysis of the aligned data, plus centroid size indicates that taxa are usually diagnosable: When a random half of the data is used to train the discriminant function, the error rate in assigning specimens in the remaining, evaluation data set to species is only 4%, compared to 3% in the training data set itself. The vast majority of classification errors are between two closely-related species pairs: *D. melanogaster* and *simulans*, and *algonquin* and *athabasca* in sub-genus *Sophophora*. *D. robusta* and *hydeii* in subgenus *Drosophila* are also frequently confused, despite being less closely related. The wide taxonomic sampling in our data set suggests that a randomly chosen set of species would be less diagnosable.

Ordination of the data along the first and third linear discriminant axes is shown in Fig. 6. The first and third axes explain 33 and 13% of the variation respectively. The second

discriminant axis (which explains 20% of the variation) is not shown, as it largely serves to separate the divergent *D. guttifera* from the other species. Examination of the ordination shows some support for the major hypothesized species groups. In this projection, subgenus *Sophophora* and the virilis-repleta clade of subgenus *Drosophila* are reasonably tightly grouped. The hypothesized *immigrans* clade, however, is spread across the entire space. In particular *D. guttifera* is very far removed from other members of this clade.

This impression is confirmed when the species are clustered based on the aligned landmark data, as shown in Fig. 7. Most members of the sub-genus *Sophophora* cluster together, with the exception of *D. willistoni*. *D. busckii* from subgenus *Dorsilopha* also clusters with the Sophophorans. The very closely related pairs (*D. melanogaster* and *simulans*, and *algonquin* and *athabasca*) are also very similar in wing shape. The virilis-repleta clade is also grouped together in general, although in this case with interlopers *Z. sepsoides* and *D. falleni*. The more closely related taxa in this clade are not generally most similar in wing shape. As in the discriminant projection, the *immigrans* clade is not recovered in the cluster analysis, with representatives scattered across the dendrogram. The two *Scaptodrosophila* group together.

Overall, the results suggest that wing shape retains a good deal of phylogenetic structure, but with cases of marked discordance. The case of *D. guttifera* is particularly suggestive, as it is one of few continental *Drosophila* species with marked wings (a series of 11 small melanized spots scattered along the long veins). Perhaps sexual selection is responsible both for these display traits and for the very unusual shape of wings in this species. On the other hand *D. nebulosa* also has melanized wings, but a typical wing shape. *D. willistoni* has very unusual wings for the otherwise conservative sub-genus *Sophophora*. Careful study of the speciose

willistoni subgroup may suggest hypotheses about the causes of its divergent wing shape.

Convergence in wing form is suggested by the similarity of phylogenetically distant taxa, such as *D. busckii* grouping within the Sophophorans.

SELECTION ON WING SHAPE

Wing size or shape has long been a popular target for artificial selection experiments (e.g. Reeve and Robertson, 1953; Waddington, 1953) due to the relative ease with which wings can be measured. For measurement of simple characters, such as length, our automated system offers few advantages. For some questions, however, it is advantageous to be able to readily construct complex selection indices that capture many aspects of variation. For example, to test whether arbitrary aspects of form can respond to selection, Weber (Weber, 1990, 1992) selected on six ratios of lengths between landmarks on the wing. Remarkably, all six ratios were readily able to evolve away from the allometric relationship they showed within species. The spline models we fit to each wing allow the instantaneous calculation of any function of wing shape.

As part of an experiment to assess the role of epistasis in evolution, we are using the WINGMACHINE system to select on a complex index of wing shape. The base population for this experiment is the IV laboratory population (Houle and Rowe, 2003). For the purposes of this experiment, we needed to select on two initially uncorrelated but highly heritable traits. To choose appropriate traits, we obtained wing data from parents and offspring of 57 full-sib families (N=470 offspring). Exploratory analyses of a variety of shape measures in this population suggested a suitable pair of traits.

Trait S_1 is defined as the standardized average distance between veins L3 and L4 distal to the proximal crossvein. See Fig. 2a for the vein terminology used. Veins L3 and L4 lie on either side of the anterior/posterior compartment boundary, the origin of morphogens that structure the development of the wing (Held, 2002). To calculate S_1 , we took ten evenly spaced points along the length of L3 distal to the crossvein, and solved for the distance to the closest point on L4. The average of these distances was then standardized by wing area. Trait S_2 is the average of the distance that the crossvein lies along long veins L4 and L5, standardized by the total length of that vein. The crossveins are determined relatively late in disk development, and involve genes different than those that set up the A-P boundary that may affect S_1 (Held, 2002). S_1 and S_2 are therefore probably affected by different developmental processes. Traits S_1 and S_2 had high heritabilities (0.54 ± 0.05 ; 0.64 ± 0.06 respectively) and additive genetic coefficients of variation typical of those found in fly wings (1.5% and 1.6%; Houle, 1992). As expected given their different developmental origins, S_1 and S_2 have a non-significant additive genetic correlation ($r_A = 0.12$).

The selection index used for artificial selection was $I = 2.6S_1 + S_2$. S_1 was weighted 2.6 times as much in the index as S_2 so that the intensity of selection on each trait would be equal. We formed two replicate populations by a random division of flies in the IV population, then founded three treatments in each replicate: selection up, selection down, and a control. Each generation, in each of the four selected treatment/replicate combinations 100 virgin flies were measured, and the 20 most extreme chosen as parents of the next generation.

Figure 8 shows the highly significant 15 S. D. divergence in trait values achieved between these selected lines in 15 generations. The realized h^2 for the selection index averaged over

treatments and replicates was 0.38, lower than that in the base population. Examination of Fig. 8 shows that this is due to a combination of asymmetry between selected directions (Down responded at a rate less than Up), and reduction in response with increasing number of generations in the Up lines.

DISCUSSION

Our automated wing analysis system WINGMACHINE, successfully fulfils its intended purpose as a means of rapidly gathering repeatable high-dimensional phenotypic data. We have shown that the system is useful for characterizing variation among *Drosophilid* species, and that it facilitates artificial selection experiments on complex aspects of wing shape.

Dryden and Mardia (1998) divide image analysis into “low” and “high-level” operations. Low level analysis involves local operations on small numbers of pixels, such as filters and edge detection. High level analysis involves detection and fitting of large-scale features of an image. Sophisticated Bayesian high-level analysis is becoming common in bio-medical imaging (Dryden and Mardia, 1998, Chapter 11). Our use of an *a priori* model of wing shape that is deformed to optimize fit to each image is a simple example of high-level analysis.

Prior to developing this approach, we devoted considerable effort to developing a feature extraction system based entirely on low level analysis. These efforts were frustrated by several aspects of wings. The leading veins are thick and exhibit high contrast, while the trailing edge of the wing does not. Second, lighting across the image is uneven. Third, small flaws in the image, such as dust or hairs, or in the wing itself, such as small nicks, are hard to automatically

disentangle from wing features. All of these frustrate simple edge detection and tracing algorithms. WINGMACHINE successfully splines wings that are both damaged and dirty. Similar complications are common in most biological imaging problems. Our success in implementing high-level analysis suggests that it could be useful in a large number of image analysis applications in basic biology.

More specifically, our approach may be directly extensible to other objects that can be summarized as a framework of intersecting lines, such as leaf veins and edges, scales or feathers. The specification of a model with different vein or edge topologies than in *Drosophila* wings is readily accomplished. While the precise low and high-level fitting algorithms in our software are specifically tailored to *Drosophila* wings, we are optimistic that these could be modified to fit models of very different structures.

In comparison with the more widely used hand-digitization of wing landmarks (e.g. Zimmerman et al, 2000; Klingenberg and Zaklan 2000) the WINGMACHINE approach has the advantage of great speed, both in handling the specimens, and recovering quantitative information from them. An experienced operator spends on average about 1 minute per specimen in total. This speed comes with some disadvantages. While the repeatabilities of most landmarks are quite high, human observers can in some cases do much better. If the goal is to characterize the mean of a population (such as a family or a species), there is a simple tradeoff between speed and accuracy: if it takes x times as long to measure an image by hand, then it will be worthwhile to do so if the measurement error of the automated system is greater than x times the measurement error achieved by hand.

The structure of the model chosen for fitting and the details of image processing

determine the precise locations of the curves and intersections recovered. The result is that the landmarks, for example, are frequently not as a human observer would place them. For example point 3 (see Fig. 3 for definition of landmarks) is repeatably placed on the wing margin just above the intersection with L3, while point 2 is placed directly at the intersection of L4 and the margin. Point 11, the intersection of L2 and L3 has relatively low repeatability because it is recognized as the intersection of the curves along these veins, rather than as the sinus formed by the interior outline of the veins, as a human observer would naturally do. This feature of the model potentially creates bias if a particular feature of the wing is of primary interest.

A third disadvantage is that the WINGMACHINE may fail for wings of species with highly melanized spots at vein intersections, for example the “picture-winged” Hawaiian *Drosophila*. Initial attempts to spline wings of *D. grimshawi* have such a high error rate that hand-digitization is simpler and less time-consuming. On the other hand, melanization seems to be dependent on rearing conditions, and we have had good success with lighter individuals of another picture-winged species, *D. gymnobasis*.

Ultimately, our understanding of biological systems needs to encompass the relationships between molecular and phenotypic data. Much attention is now focused on high throughput genomic techniques such as sequencing, expression microarrays and proteomics. To take advantage of this avalanche of genetic data, comparable efforts will be needed to characterize the whole-organism phenotype, what might be called phenomics (Houle, 2001). The WINGMACHINE is an example that serves to illustrate both that phenome level efforts are possible, and just how far short of comprehensive knowledge they fall.

ACKNOWLEDGEMENTS

Feng Lu deserves all credit for developing the FINDWING program. If only he hadn't disappeared. Y. Ng and V. Jackson wrote the program SELECTOR. F. James Rohlf generously modified his TPS programs to facilitate our analyses, and responded to all queries on how to use them. L. Rowe, D. Jackson, T. Dickinson and D. Currie offered valuable advice. D. Houle was supported by NSERC, and by NSF grant DEB-0129219. P. Galpern was supported by a PGS award from NSERC. L. Carpenter, M. Castilla, J. Gunzburger, N. Guram, Y. Ng, F. Smyth, J. Woehlke, and T. Weier, all helped measure wings.

REFERENCES

- ACD Systems. 2001. ACDSsee 4.0. ACD Systems, Inc. (www.acdsystems.com), Saanichton, BC.
- Cowley, D. E., W. R. Atchley, and J. J. Rutledge. 1986. Quantitative genetics of *Drosophila melanogaster*. I. Sexual dimorphism in genetic parameters for wing traits. *Genetics* 114:549-566.
- Dickinson, M. H., S. Hannaford, and J. Palka. 1997. The evolution of insect wings and their sensory apparatus. *Brain Behav. Evol.* 50:13-24.
- Dryden, I. L., and K. V. Mardia. 1998. *Statistical Shape Analysis*. John Wiley and Sons, Chichester.
- Ferson, S., F. J. Rohlf, and R. K. Koehn. 1985. Measuring shape variation of two-dimensional outlines. *Syst. Zool.* 34:59-68.
- Garcia-Bellido, A., and J. F. de Celis. 1992. Developmental genetics of the venation pattern of *Drosophila*. *Ann. Rev. Genet.* 26:277-304.
- Gilchrist, A. S., R. B. R. Azevedo, L. Partridge, and P. O'Higgins. 2000. Adaptation and constraint in the evolution of *Drosophila melanogaster*. *Evolution and Development* 2:114-124.
- Held, L. I., Jr. 2002. *Imaginal Discs: The Genetic and Cellular Logic of Pattern Formation*. Cambridge, Cambridge.
- Houle, D. 1992. Comparing evolvability and variability of quantitative traits. *Genetics* 130:195-204.
- Houle, D. 2001. Characters as the units of evolutionary change. Pages 109-140 *in* *The Character Concept in Evolutionary Biology* (G. P. Wagner, ed.). Academic Press, New York.
- Houle, D., and L. Rowe. 2003. Natural selection in a bottle. *Am. Nat.* 161:50-67.
- Insightful Corporation. 2001a. S-Plus 6.0 Professional Release 1. Insightful, Seattle.
- Insightful Corporation. 2001b. S-Plus 6 for Windows Programmer's Guide. Insightful, Seattle.

- Jensen, R. J., K. M. Ciofani, and L. C. Miramontes. 2002. Lines, outlines, and landmarks: morphometric analyses of leaves of *Acer rubrum*, *Acer saccharinum* (Aceraceae) and their hybrid. *Taxon* 51:475-492.
- Klingenberg, C. P., and S. D. Zaklan. 2000. Morphological integration between developmental compartments in the *Drosophila* wing. *Evolution* 54:1273-1285.
- Littell, R. C., G. A. Miliken, W. W. Stroup, and R. D. Wolfinger. 1996. SAS System for Mixed Models. SAS Institute, Cary, NC.
- Liu, J., J. M. Mercer, L. F. Stam, G. C. Gibson, Z.-B. Zeng, and C. C. Laurie. 1996. Genetic analysis of a morphological shape difference in the male genitalia of *Drosophila simulans* and *D. mauritiana*. *Genetics* 142:1129-1145.
- Lu, F. 1997. FINDWING: Drosophilid spline fitting software. Dept. of Computer Science, University of Toronto.
- Lu, F., and E. E. Milios. 1994. Optimal spline fitting to planar shape. *Signal Processing* 37:129-140.
- Media Cybernetics. 1999. ImagePro Plus, Version 4.0 for Windows. Media Cybernetics (www.mediacy.com), Silver Spring, MD.
- Mezey, J., and D. Houle. 2003. Dimensionality of wing shape in *Drosophila melanogaster*. *Nature* submitted.
- O'Grady, P. M., and M. G. Kidwell. 2002. Phylogeny of the subgenus *Sophophora* (Diptera:Drosophilidae) based on combined analysis of nuclear and mitochondrial DNA sequences. *Mol. Phyl. Evol.* 22:442-453.
- Powell, J. R., and R. DeSalle. 1995. *Drosophila* molecular phylogenies and their uses. Pages 87-138 in *Evolutionary Biology*, Vol. 28 (M. K. Hecht, R. J. MacIntyre, and M. T. Clegg, eds.).

- Plenum Press, New York.
- Reeve, E. C., and F. W. Robertson. 1953. Studies in quantitative inheritance II. Analysis of a strain of *Drosophila melanogaster* selected for long wings. *J. Genet.* 51:276-316.
- Remsen, J., and P. O'Grady. 2002. Phylogeny of Drosophilinae (Diptera: Drosophilidae), with comments on combined analysis and character support. *Mol. Phyl. Evol.* 24:249-264.
- Rohlf, F. J. 1993. Feature extraction in systematic biology. Pages 375-392 in *Advances in computer methods for systematic biology: artificial intelligence, databases, computer vision* (R. Fortuner, ed.). Johns Hopkins, Baltimore.
- Rohlf, F. J. 1998a. tpsDig: digitizing software. V. 1.17. <http://life.bio.sunysb.edu/morph/>. Dept. of Ecology and Evolution, State University of New York, Stony Brook, NY.
- Rohlf, F. J. 1998b. tpsRegr: shape regression. V. 1.17. <http://life.bio.sunysb.edu/morph/>. Dept. of Ecology and Evolution, State University of New York, Stony Brook, NY.
- Rousseeuw, P. J. 1985. Multivariate estimation with high breakdown point. Pages 283-297 in *Multivariate Statistics and Applications* (W. Grossman, G. Pflug, I. Vincze, and W. Wertz, eds.). Reidel, Dordrecht.
- Rousseeuw, P. J., and B. C. van Zomeren. 1990. Unmasking multivariate outliers and leverage points. *J. Am. Stat. Assoc.* 85:633-639.
- SAS Institute. 2002. The SAS System for Windows, Release 8.01. SAS, Cary, NC.
- Scion Corporation. 2001. Scion Image 2.0. Scion (www.scioncorp.com), Frederick, MD.
- Stark, J., J. Bonacum, J. Remsen, and R. DeSalle. 1999. The evolution and development of Dipteran wing veins: a systematic approach. *Ann. Rev. Entomol.* 44:97-129.
- Tatarenkov, A., and F. J. Ayala. 2001. Phylogenetic relationships among species groups of the

- virilis-repleta* radiation of *Drosophila*. Mol. Phyl. Evol. 21:327-331.
- Waddington, C. H. 1953. Genetic assimilation of an acquired character. Evolution 7:118-126.
- Weber, K. E. 1988. A system for rapid morphometry of whole, live flies. Drosop. Inform. Serv. 67:96-101.
- Weber, K. E. 1990. Selection on wing allometry in *Drosophila melanogaster*. Genetics 126:975-989.
- Weber, K. E. 1992. How small are the smallest selectable domains of form? Genetics 130:345-353.
- Weber, K. E., and L. T. Diggins. 1990. Increased selection response in larger populations. II. Selection for ethanol vapor resistance in *Drosophila melanogaster* at two population sizes. Genetics 125:585-597.
- Weeks, P. J. D., and K. J. Gaston. 1997. Image analysis, neural networks, and the taxonomic impediment to biodiversity studies. Biodiversity and Conservation 6:263-274.
- Zhou, Y., L. Ling, and F. J. Rohlf. 1985. Automatic description of the venation of mosquito wings from digitized images. Syst. Zool. 34:346-358.
- Zimmerman, E., A. Palsson, and G. Gibson. 2000. Quantitative trait loci affecting components of wing shape in *Drosophila melanogaster*. Genetics 155:671-683.

Table 1. Repeatabilities of centroid size and landmark positions in the Wabasso population of *Drosophila melanogaster*. Centroid size is in units of μm . Point locations are in units of mean centroid size/1000.

Trait	Difference ^a ♀ - ♂	Among fly variance ^b	Percent of within-sex variance		
			Over repeated imaging %	Operator	Over fitting, models % Fly
Centroid size	164.83	517.21	96.2	0.5	99.5
Landmark: 1	3.32	52.67	90.2	1.1 ***	97.4
2	6.83	22.54	91.1	0.0	96.7
3	4.18	21.78	89.5	0.3 *	96.7
4	11.68	75.15	91.6	0.9 ***	96.1
5	3.44	14.32	46.9	2.4 *	72.6
6	3.16	11.71	75.7	3.2 ***	94.6
7	4.60	39.82	94.3	0.2 **	97.8
8	2.19	43.83	95.2	0.2 ***	98.0
9	1.42	24.57	90.6	0.9 ***	96.3
10	2.61	26.74	91.7	0.4 ***	97.5
11	2.17	7.67	64.5	1.6 ***	78.7
12	4.08	12.39	65.8	0.6 ***	71.0
Landmark total		355.17	86.0	0.8	92.7

* $P < 0.05$; ** $P < 0.01$; *** $P < 0.001$.

^aDistance between mean locations of each point. All differences between the sexes are significant at $P < 0.0001$.

^bAll among fly differences are significant at $P < 0.0001$. Point variances are the sums of variance components in the x and y dimensions.

Table 2. Taxa included in the multi-species data set. Genus designations follow the stock list of the Tucson *Drosophila* Species Stock Center (<http://stockcenter.arl.arizona.edu/>).

Genus (subgenus)	species	Code	Collection Locale	Stock No.	N
<i>Drosophila (Sophophora)</i>	<i>algonquin</i>	ALG	Toronto, Ontario, Canada	–	64
<i>Drosophila (Sophophora)</i>	<i>athabasca</i>	ATH	Toronto, Ontario, Canada	–	76
<i>Drosophila (Sophophora)</i>	<i>melanogaster</i>	MEL	See text	–	192
<i>Drosophila (Sophophora)</i>	<i>simulans</i>	SIM	Toronto, Ontario, Canada	–	114
<i>Drosophila (Sophophora)</i>	<i>nebulosa</i>	NEB	San Jose, Costa Rica	14030-0761.1	97
<i>Drosophila (Sophophora)</i>	<i>willistoni</i>	WIL	Royal Palm Pk., Florida, USA	14030-0811.2	88
<i>Drosophila (Sophophora)</i>	<i>sturtevanti</i>	STU	Montecristi, Dominican Rep.	14043-0871.11	102
<i>Drosophila (Sophophora)</i>	<i>saltans</i>	SAL	San Jose, Costa Rica	14045-0911.0	104
<i>Drosophila (Drosophila)</i>	<i>virilis</i>	VIR	Pasadena, California, USA	15010-1051.0	109
<i>Drosophila (Drosophila)</i>	<i>americana americana</i>	AME	Millersburg, P.A., USA	15010-0951.3	113
<i>Drosophila (Drosophila)</i>	<i>hydeii</i>	HYD	Toronto, Ontario, Canada	–	180
<i>Drosophila (Drosophila)</i>	<i>repleta</i>	REP	Barbados	15084-1611.0	108

Table 2, continued.

Genus (subgenus)	species	Code	Collection Locale	Stock No.	N
<i>Drosophila (Drosophila)</i>	<i>micromelanica</i>	MIC	Santa Rita Mts., Arizona, USA	15030-1151.0	31
<i>Drosophila (Drosophila)</i>	<i>robusta</i>	ROB	Lake Champlain, Vermont, USA	15020-1111.1	108
<i>Drosophila (Drosophila)</i>	<i>falleni</i>	FAL	Toronto, Ontario, Canada	–	95
<i>Drosophila (Drosophila)</i>	<i>guttifera</i>	GUT	Austin, Texas, USA	15130-1971.0	103
<i>Drosophila (Drosophila)</i>	<i>immigrans</i>	IMM	Tofino, B.C., Canada	–	101
<i>Drosophila (Drosophila)</i>	<i>sulfurigaster</i>	SUL	Kuala Lumpur, Malaysia	15112-1811.0	109
<i>Drosophila (Dorsilopha)</i>	<i>busckii</i>	BUS	Tofino, B.C., Canada	–	101
<i>Hirtodrosophila</i>	<i>pictiventris</i>	PIC	Great Inagua Is., Bahamas	12000-0072.0	113
<i>Zaprionus</i>	<i>inermis</i>	ZIN	Koutaba, Cameroun	50000-2746.0	12
<i>Zaprionus</i>	<i>sepsoides</i>	ZSE	unknown	50000-2744.0	21
<i>Chymomyza</i>	<i>procnemis</i>	CPR	Oahu, Hawaii, USA	20000-2631.1	106
<i>Scaptodrosophila</i>	<i>stoneii</i>	STO	Tehran, Iran	11010-0041.0	44
<i>Scaptodrosophila</i>	<i>lebanonensis casteeli</i>	LEB	Veyo, Utah, USA	11010-0011.0	98

FIGURE CAPTIONS

Fig. 1. Wing grabber. (a) Separated into components; (b) cross-section of assembled grabber.

Fig. 2. Steps in image processing. Raw image (a) is reversed, then filtered to minimize background features (b), then thresholded, and holes filled (c), features are skeletonized (reduced to 1 pixel width) (d) and short segments pruned away (e). The intersections of these lines are used to register the model with this image, and the model modified to fit the grey scale image in (c). The final result with the spline model overlaid on it (f). The white circles are the two landmarks digitized by the operator. Wing is from the Wabasso population of *D. melanogaster*.

Fig. 3. A B-spline wing model. Circles are the ends of splines, and the large filled circles are the landmarks analyzed. The squares are the internal control points of the splines. The long veins are labeled according to the standard ‘genetic’ nomenclature used in the paper. The model is optimized for a wing of *Drosophila affinis*.

Fig. 4. Phylogenetic hypothesis for the taxa in this study.

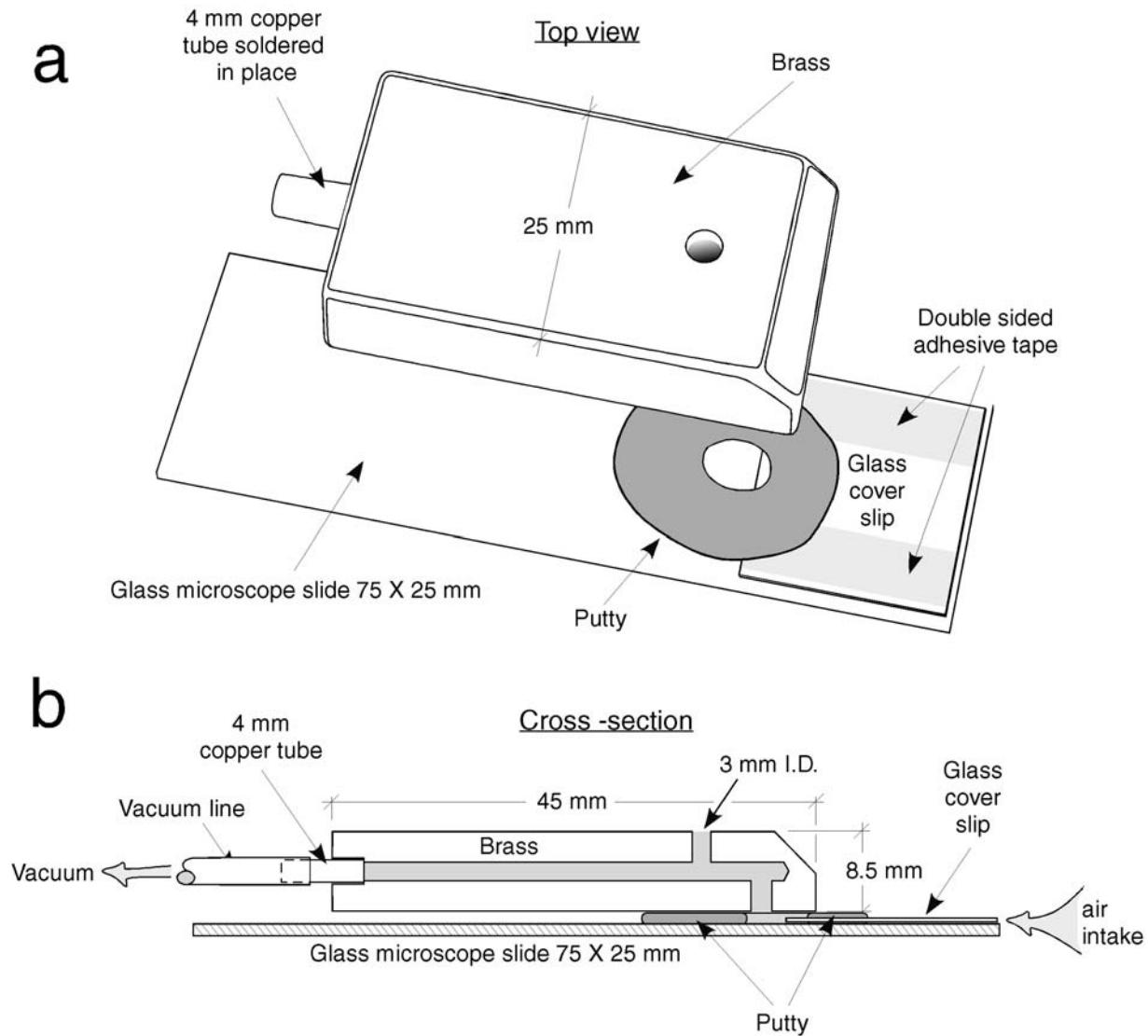
Fig. 5. Aligned species data. Black circles represent the mean locations of landmarks in each species; grey dots are the positions of each of the landmarks in each of the 2406 specimens. The wing used as the basis for the line drawing was chosen to be as close as possible to the tangent or reference configuration.

Fig. 6. Ordination of species data on the first and third discriminant axes. Gray dots are individuals, while large symbols denote species means.

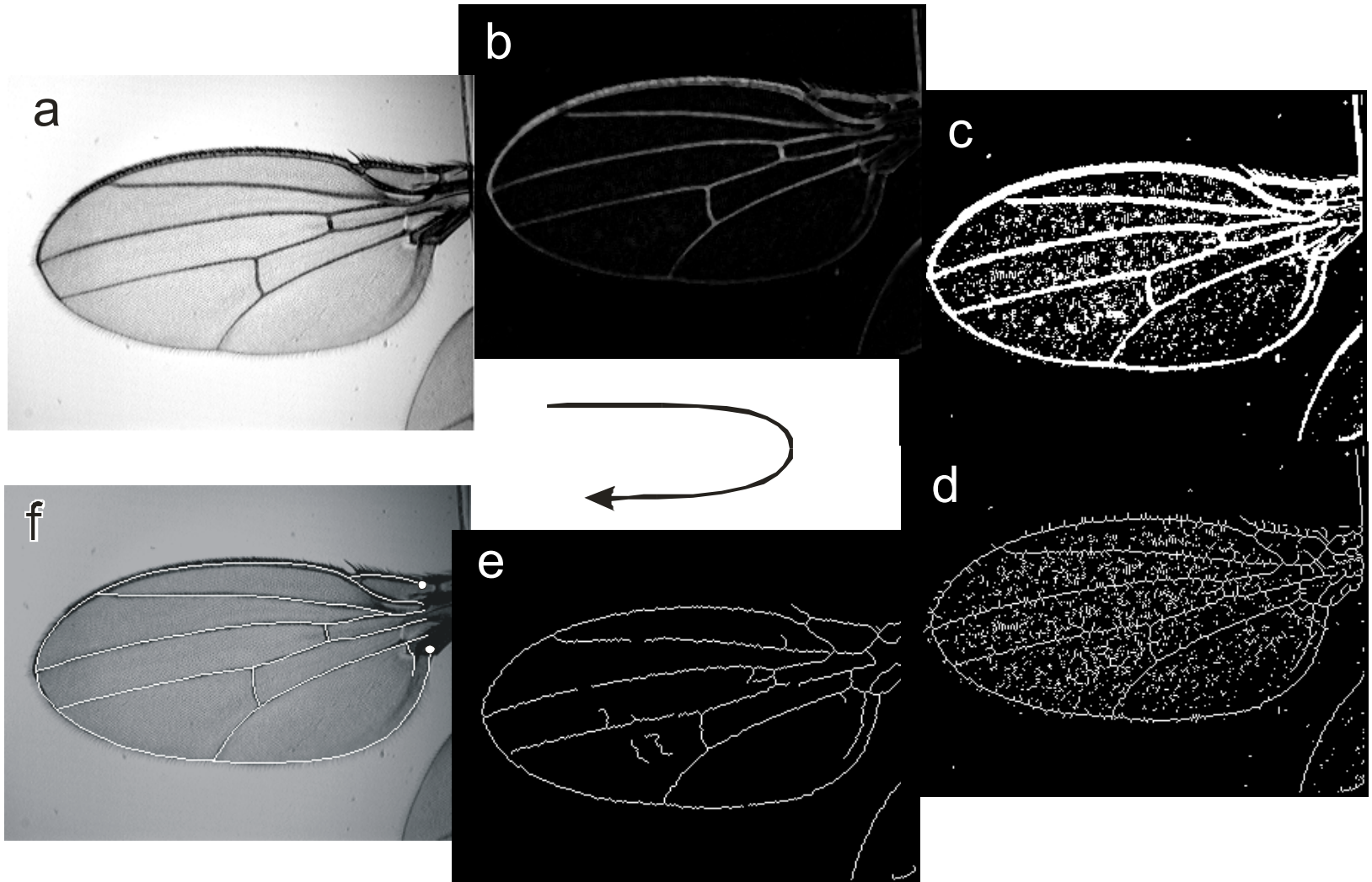
Fig. 7. UPGMA dendrogram of taxa based on mean wing shape.

Fig. 8. Response to 14 generations of selection on the wing shape index. Two replicate populations were selected up, and two were selected down. Wings of female flies from an up-selected (upper) and down-selected (lower) population at generation 14 are shown.

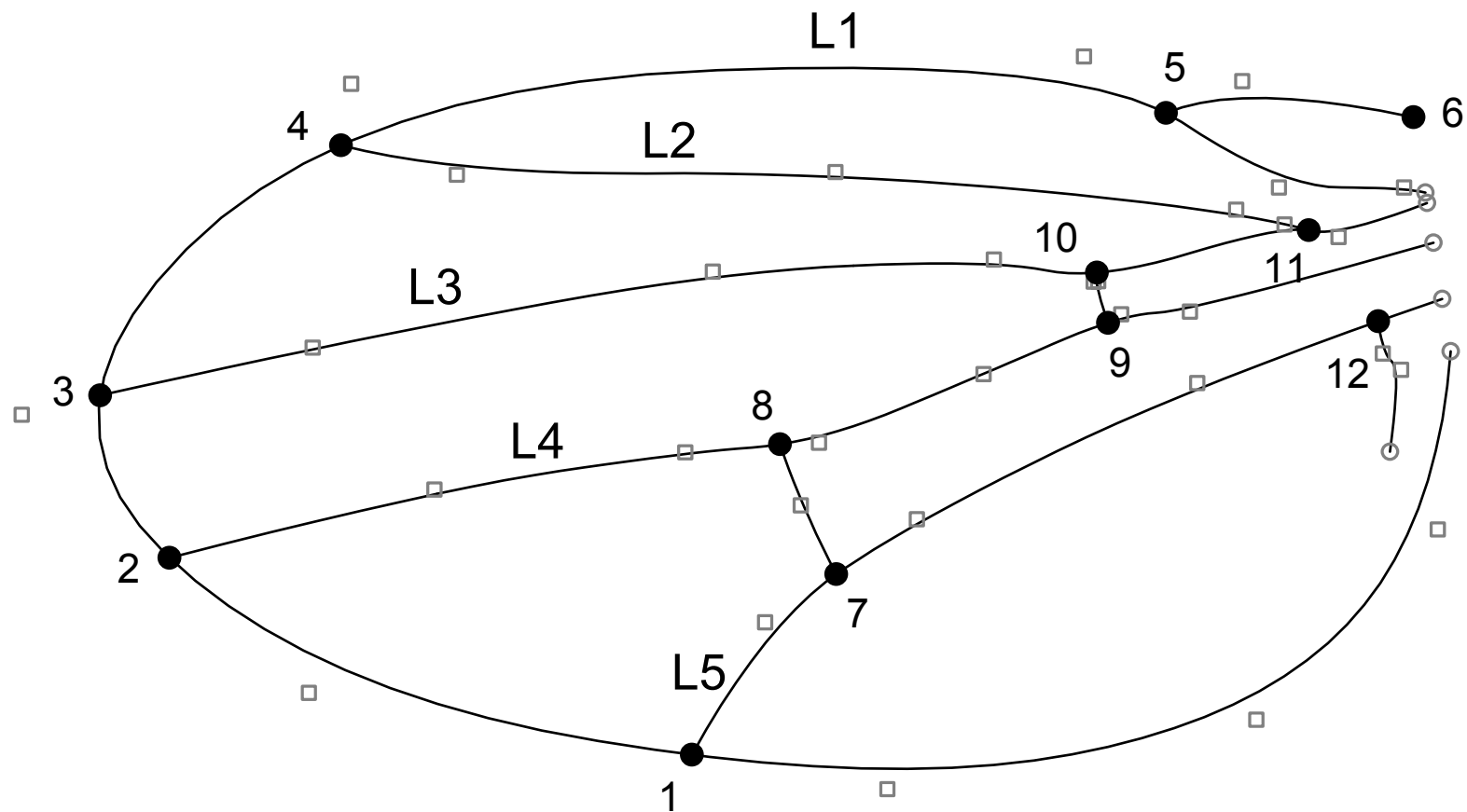
Houle et al. Fig. 1. Wing grabber. (a) Separated into components; (b) cross-section of assembled grabber.



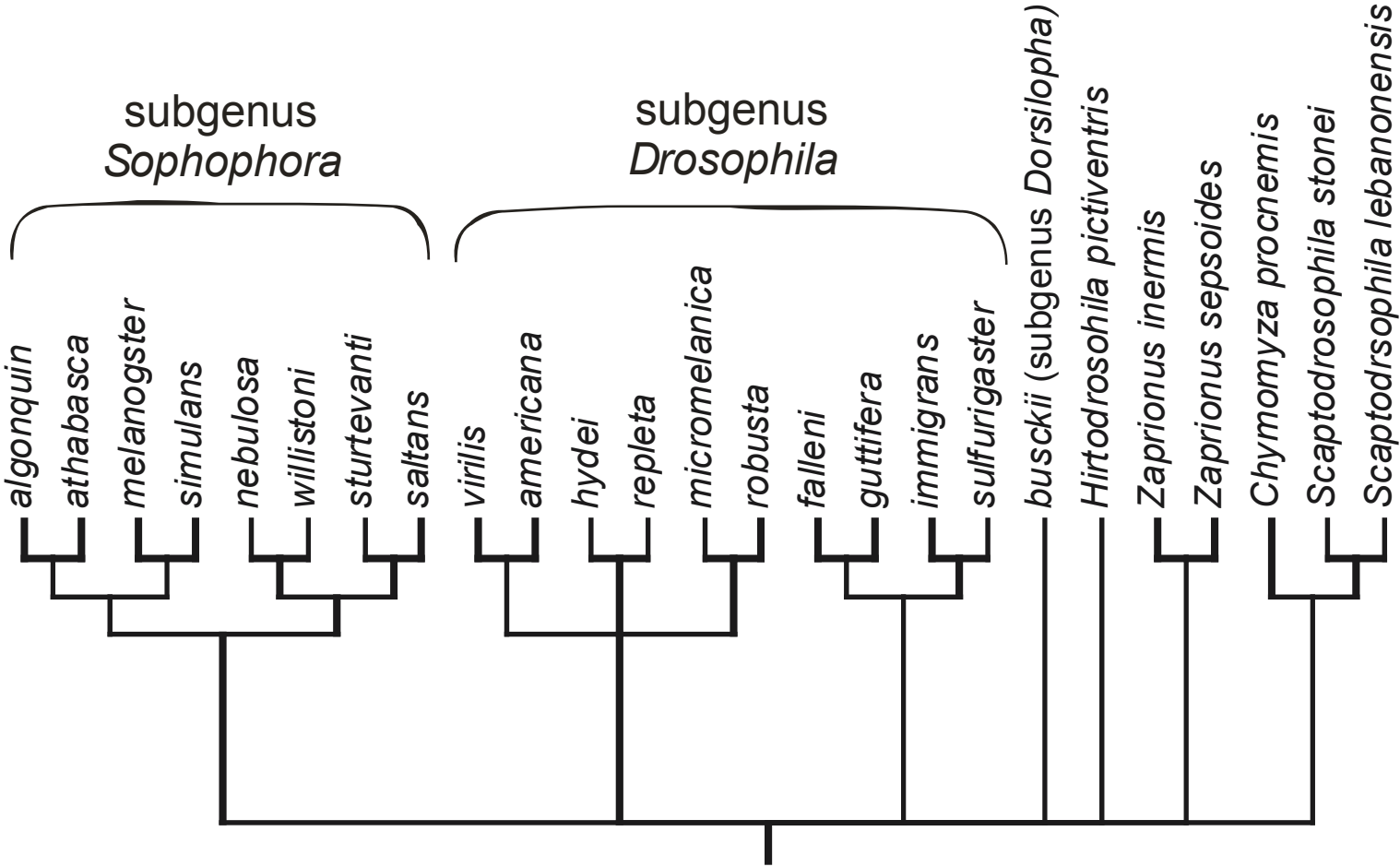
Houle et al. Fig. 2 Steps in image processing. Raw image (a) is reversed, then filtered to minimize background features (b), then thresholded, and holes filled (c), features are skeletonized (reduced to 1 pixel width) (d) and short segments pruned away (e). The intersections of these lines are used to register the model with this image, and the model modified to fit the grey scale image in (c). The final result with the spline model overlaid on it (f). The white circles are the two landmarks digitized by the operator. Wing is from the Wabasso population of *D. melanogaster*.



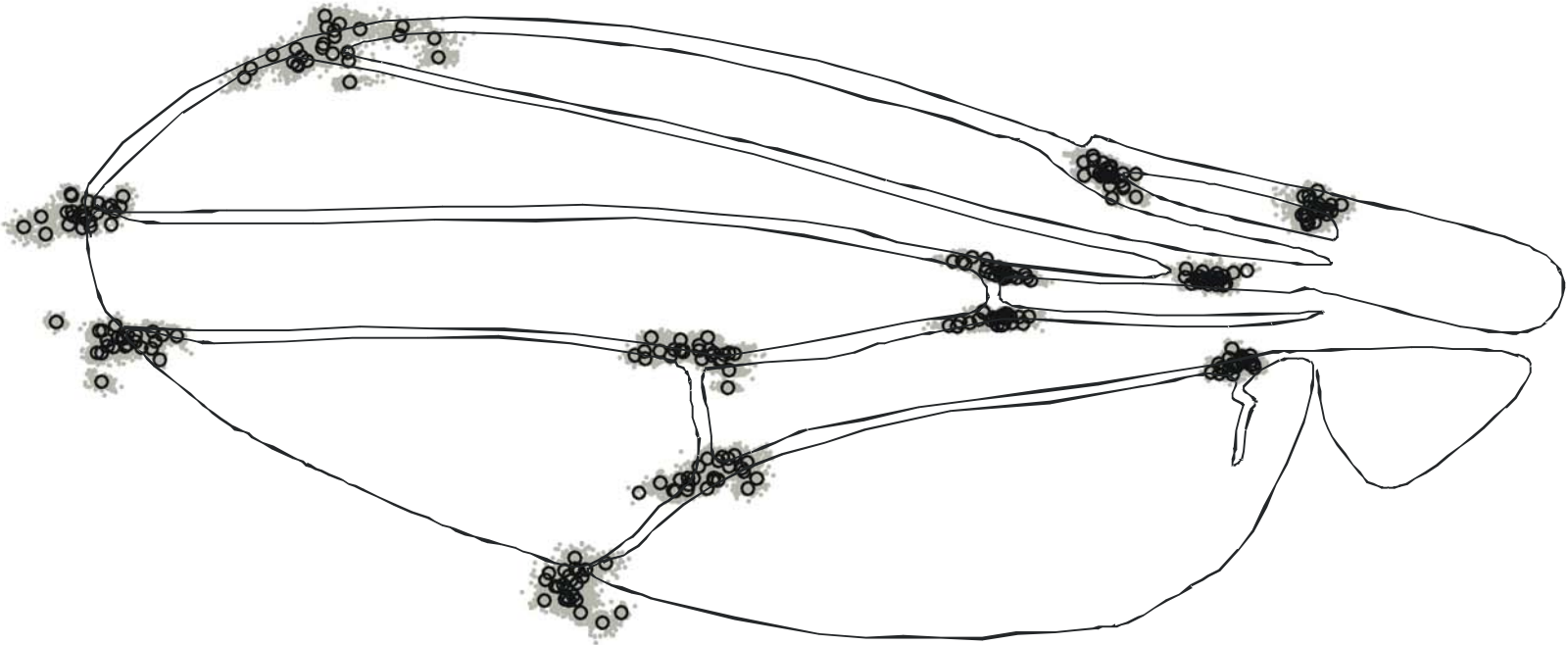
Houle et al. Fig. 3. A B-spline wing model. Circles are the ends of splines, and the large filled circles are the landmarks analyzed. The squares are the internal control points of the splines. The long veins are labeled according to the standard 'genetic' nomenclature used in the paper. The model is optimized for a wing of *Drosophila affinis*.



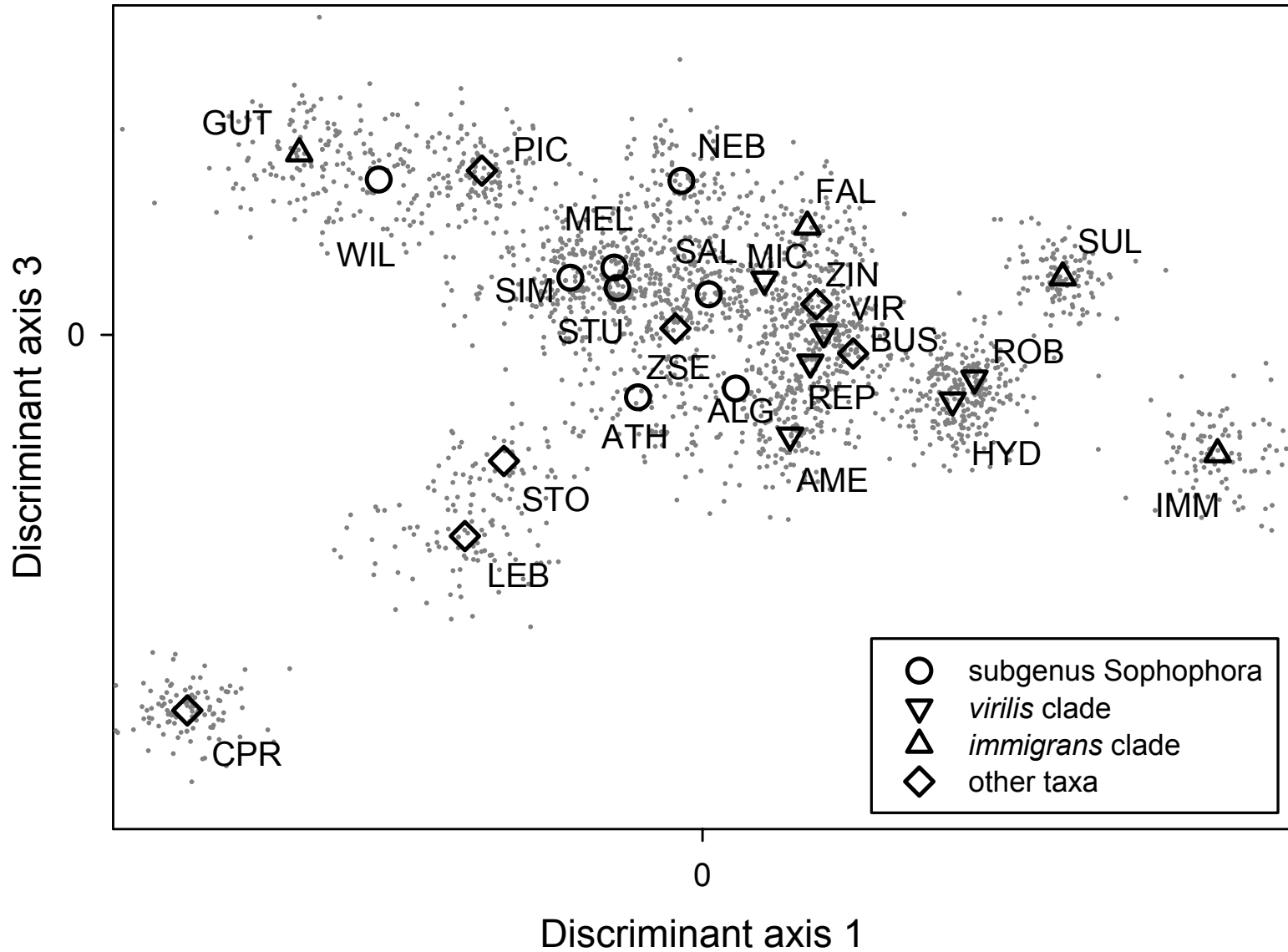
Houle et al. Fig. 4. Phylogenetic hypothesis for the taxa in this study.



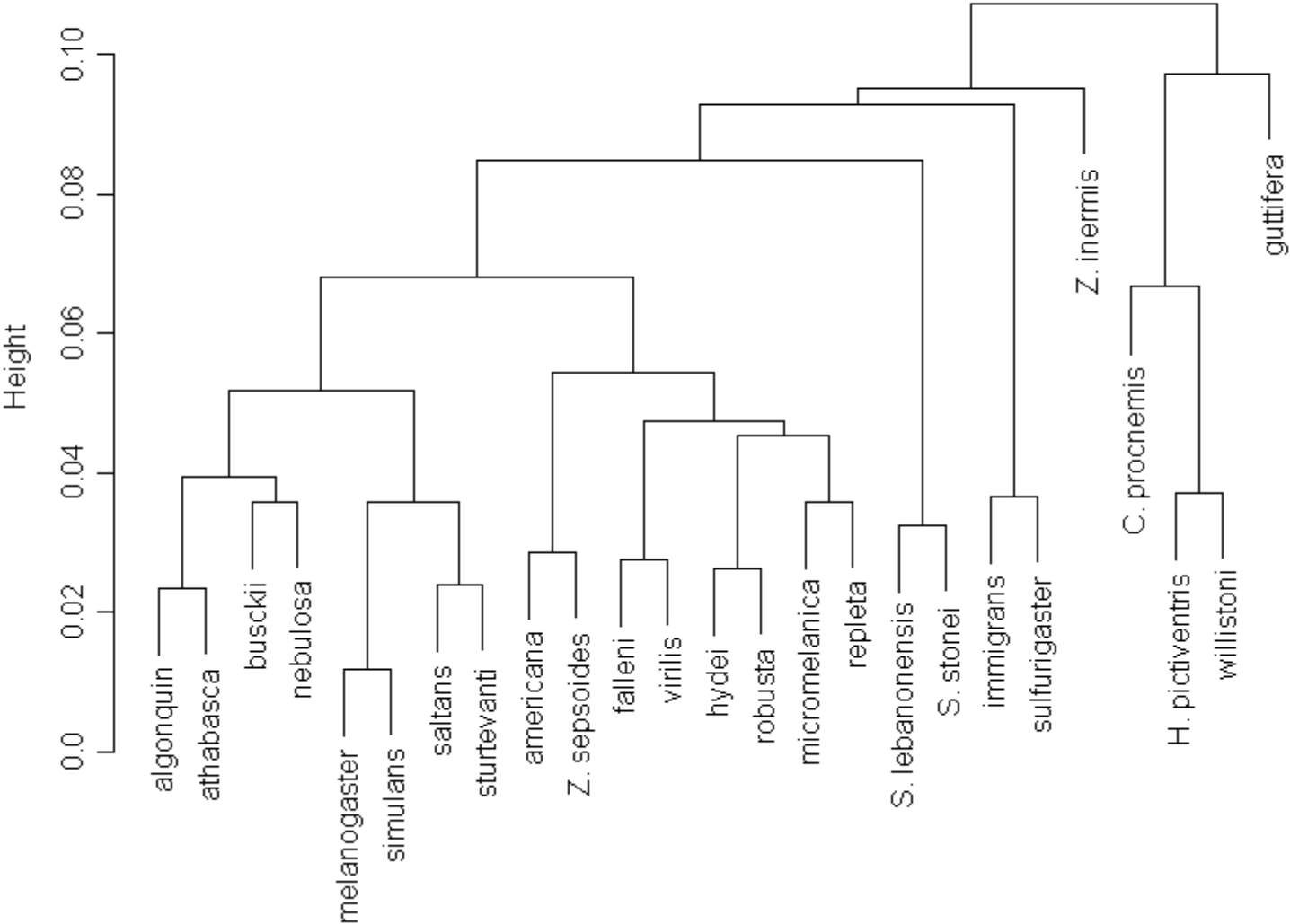
Houle et al. Fig. 5. Aligned species data. Black circles represent the mean locations of landmarks in each species; gray dots are the positions of each of the landmarks in each of the 2406 specimens. The wing used as the basis for the line drawing was chosen to be as close as possible to the tangent or reference configuration.



Houle et al. Fig. 6. Ordination of species data on the first and third discriminant axes. Gray dots are individuals, while large symbols denote species means.



Houle et al. Fig. 7. UPGMA dendrogram of taxa based on mean wing shape.



Houle et al. Fig. 8. Response to 14 generations of selection on the wing shape index. Two replicate populations were selected up, and two were selected down. Wings of female flies from an up-selected (upper) and down-selected (lower) population at generation 14 are shown.

